Am J Transl Res 2021;13(12):13471-13484
www.ajtr.org /ISSN:1943-8141/AJTR0134697

Original Article

Comparative analysis identifies significant peptides related to asthma mechanism

Danying Zhu[1*], Chao Wang[1*], Chaoyue Meng[1], Yiwen Liu[2], Zeyu Zeng[1], Ran Zhao[1], Xiaoyan Dong[1], Xingyun Wang[2]

[1]*Department of Respiratory, Shanghai Children's Hospital, Shanghai Jiao Tong University, Shanghai 200062, China;* [2]*Hongqiao International Institute of Medicine, Tongren Hospital, Shanghai Jiao Tong University School of Medicine, Shanghai 200336, China.* [*]*Equal contributors.*

Received April 26, 2021; Accepted September 9, 2021; Epub December 15, 2021; Published December 30, 2021

Abstract: Asthma is a kind of chronic inflammatory and allergic disease. Peptides have showed significant potential for asthma therapeutics. Our study aims to identify the differential peptidomic profiles between asthmatic and non-asthmatic mice. Methods and results: House dust mite (HDM) was utilized to build an asthmatic mouse model. Lung tissues were tested by histological analysis and liquid chromatography-mass spectrometry (LC-MS/MS). Histological analysis of lung tissues showed eosinophils infiltration, thickening of the bronchial wall, swelling, and hyperemia of the mucosa. In which, 108 of 1564 peptides were identified and showed significant differential expression (fold change >2 or fold change <0.5, *P*-value <0.05), containing 44 upregulated and 64 downregulated peptides. GO analysis demonstrated that the functional precursor proteins of the identified peptides were primarily associated with actin polymerization or depolymerization, receptor-mediated endocytosis (RME), and regulation of the inflammatory response. KEGG analysis revealed that the peptides were associated with soluble N-ethylmaleimide-sensitive factor attachment protein receptor (SNARE) interactions in vesicular transport, bacterial invasion of epithelial cells, and tight junction signaling pathways. Precursor proteins analysis revealed that peptides derived from glutamic acid-rich protein-like 3 (SH3BGRL3) might be related to the incidence of asthma. Conclusions: Our results provide evidence for the candidate treatment sites of peptides in asthma.

Keywords: Asthma, peptides, liquid chromatography-mass spectrometry

Introduction

Asthma is a chronic inflammatory disease that affects the airway and its global prevalence is reported to be approximately 3.6% [1]. Asthma is a heterogeneous disease that involves interactions between gene and environment [2] and iis affected by numerous types of cells [3]. Allergic asthma is the most common phenotype, which is primarily induced by sensitization to environmental allergens and mediated mainly by the Th2 immune response [4]. Th2 cells mediate immune response through producing cytokines such as IL-4, IL-5, and IL-13 [5]. Based on the pathogenesis, many interventions have been used to alleviate asthma symptoms successfully, such as inhaled bronchodilators, corticosteroid, allergen avoidance measures [6], biologic therapy (omalizumab or mepolizumab, etc.) [7]. It has been reported that small molecule peptides have therapeutic potential for asthma. Peptides drugs, such as peptide CKLF1-C19 [8], TFF [9] have provided effective treatments for relieving asthma symptoms. However, the peptides expression profile of asthma pathogenesis has not been elucidated.

We intended to identify peptidomic profiles of lung tissues and find out the evidence for peptides that participate in the pathological processes of asthma. Animal models, mostly rats and mice, have been utilized to identify the progress, pathogenesis mechanism of asthma, and new therapeutic targets for humans [10-12]. House dust mite (HDM) is a type of frequent cause of allergic asthma and a ubiquitous allergen related to humans [13] and is usually used to construct asthma animal models [14]. Here, we use HDM [11] to construct asth-

matic mouse models. We use the label-free liquid chromatography/mass spectrometry (LC-MS/MS) technique to compare different peptides of lung tissues isolated from asthmatic and non-asthmatic mice. Then GO analysis, KEGG analysis, and STRING database are utilized to characterize the differentially expressed peptides. Our study intended to provide new ideas to the mechanism of asthma and to find out new potential targets for therapeutic.

Materials and methods

Mice model of asthma

C57BL/6 mice aged 4 to 6 weeks were divided into two groups (3 per group): the HDM group and the control group. In the HDM group, intraperitoneal injection of HDM which is used for skin prick testing (80 μL, 10 HEP/ml, ALK-ABELL, Spain) were performed on day 0, day 7 and day 14, then challenged by intranasal treatment with HDM (10 μL/day) on days 15-19. The control group was treated with PBS instead of HDM. On day 20, acetylcholine spray was given to two groups at different concentrations (12.5, 25, 100 mg/ml ×2 ml, respectively). Lung tissues were lavaged with PBS after opening the thorax and endotracheal intubation. Then separated lung tissues were used for tissue sections and LC-MS/MS analysis. The animal experiments were approved by the Animal Ethical Committee of Shanghai Children's Hospital (ethic number: LLSC2019038).

Peptides extraction and purification

Lung tissues were cut into small pieces, then the tissues (1 g) were mixed with water (3 mL) and boiled for 10 min. The samples were grounded with steel beads at 50 Hz at 4°C for 10 min. Glacial acetic acid was added (1 M final concentration) and the samples were vortexed and shaken for 2 min. Next, acetonitrile was added (50% final concentration) into the samples. The supernatant was placed in a clean EP tube for freeze-drying after centrifugation at 12000 g, 4°C for 10 min. Then 80% acetone solution was added into the tube, vortexed, and sonicated in the water bath for 2 min. The supernatant was placed in another EP tube for freeze-drying after centrifugation at 20000 g, 4°C for 30 min. Then 200 μl of the 0.1% TFA solution was added into the tube, and the peptides were desalted and lyophilized.

LC/MS combination analysis

Q-Exactive Plus mass spectrometer (ThermoFisher Scientific, USA) was used for LC-MS/MS test. Peptides were performed with a C18 column (150 mm ×75 μm, 3 μm, Eksigent, USA). Mass spectrometry was conducted in positive-ion mode. The MS1 parameters were: Resolution, 70,000; automatic gain control (AGC) target, 3e6; scan range, 350-1400 m/z; 20 ions of the highest intensities were selected for MS/MS scans, the MS2 parameters were: Resolution, 17,500; AGC target, 1e6; isolation window, 1.6 m/z. For liquid chromatography separation, a C18 column (250 mm ×75 μm, 3 μm, Eksigent, USA) was used for analysis. Mobile phase A was acetonitrile with 0.1% formic acid, mobile phase B was water with 0.1% formic acid. Peptides were eluted using a 78 min gradient, the injection volume was 6 μL and the flow rate was 300 nl/min. Using the following gradient elution program: 0-45 min, 5-30% B; 45-62 min, 30-80% B; 62-67 min, 80% B; 67-68 min, 80-5% B; 68-78 min, 5% B.

HE slices preparation

Slices with a thickness of 4 μm were placed on slides incubated with 3-aminopropyltriethoxysilane. Sections were deparaffinized by xylene, then rehydrated with reduced concentrations of ethanol (100%, 95%, 85% for 5 minutes each). In citrate buffer solution (pH 6.0), hematoxylin staining for 2-5 minutes. After 0.5%-1% hydrochloric acid alcohol differentiation, sections were washed in water for about 10 minutes. Eosin staining for 2 minutes. After staining, sections were dehydrated through increasing concentrations of ethanol and xylene.

Bioinformatics analysis

ProtParam (http://web.expasy.org/protparam/) was used to calculate the isoelectric point (PI) and molecular weight (MW) of the identified peptide. GO and KEGG enrichment analysis (https://david.ncifcrf.gov/) were performed to predict the functions of the precursor proteins of the peptides. UniProt database (http://www.uniprot.org/) and STRING (http://string-db.org/) were applied for analyzing the corresponding functions of the precursor proteins and integrated into the network map.

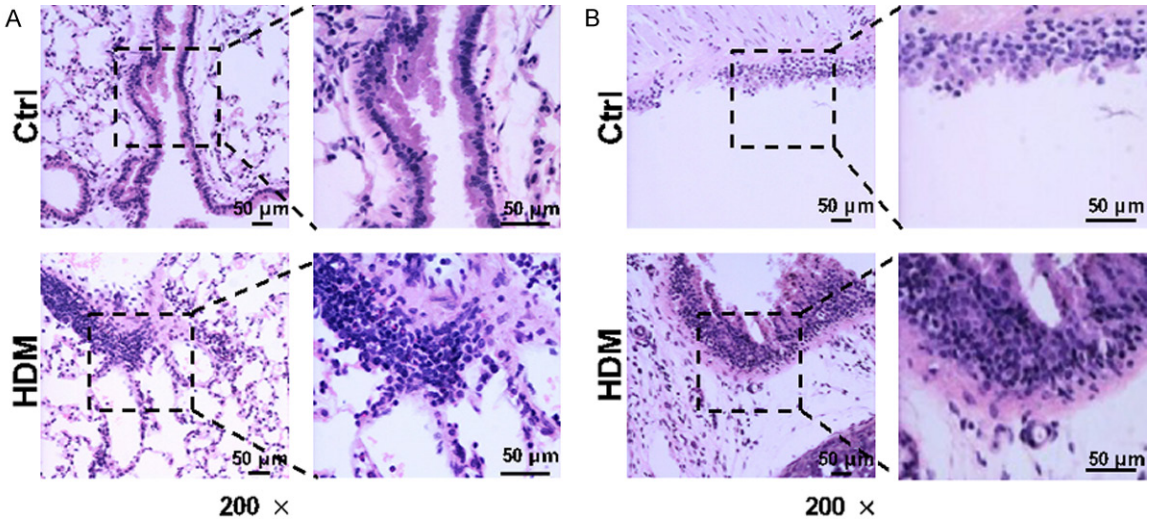

Figure 1. HE staining of lung and bronchial tube tissues of asthmatic mice. A. HE staining of lung tissues in the HDM and the control group. The used magnification was 200×. B. HE staining of bronchial tube tissues in the HDM and the control group. The used magnification was 200×. Bar =50 μm.

Western blot

Lung tissues of mice were homogenized and total proteins were extracted with 500 μl cell lysis buffer (ThermoFisher, USA) per 100 mg tissues. After centrifugation at 16000 g for 10 min at 4°C, the supernatant was transferred into a new EP tube and taken for total protein quantification. Then the samples were heat-denatured at 100°C for 5 minutes with 5× SDS-PAGE loading buffer (Beyotime, China) and fractionated on 10% SDS-PAGE gels (Epizyme, China). Following electrophoresis at 80 V for 90 min, proteins were transferred to a nitrocellulose membrane and blocked with 5% skim milk powder for one hour. GAPDH monoclonal antibody (1:20000, 60004-1-Ig, Proteintech, UK) was used as a standard control protein. E-cadherin mouse monoclonal antibody (1:2000, 60335-1-Ig, Proteintech, UK) was used as primary antibodies and incubated at 4°C overnight. Then the membranes were incubated with goat anti-mouse antiserum (1:5000, SA00001-1, Proteintech, UK). Finally, the immunoreactive bands were visualized by chemiluminescence.

Statistical analysis

Statistical comparisons were administered by Student's *t*-test. GraphPad Prism 7 software was used to visualize bioinformatics analysis results. When the *P*-value was <0.05, data were considered statistically significant.

Results

Histopathological changes of HDM-sensitized mice

HE staining was used for the assessment of pathological changes in lung tissues under a light microscope. Lung tissues from the HDM group were seriously injured, characterized by increasing eosinophils infiltration in lamina propria, basal layer and submucosa (**Figure 1A**), thickening of the bronchial wall, swelling and hyperemia of the mucosa (**Figure 1B**). While lung tissues in the control group showed a normal structure and little eosinophils infiltration.

The differential peptides between the HDM group and the control group

The extracted peptides in lung tissues from the HDM group and the control group were tested by LC-MS/MS. In which, 1564 peptides were identified. Among them, 108 peptides represent a significant increase in expression (**Table 1**) (fold change >2 or fold change <0.5, *P*-value <0.05), containing 44 upregulated peptides and 64 downregulated peptides (**Figure 2A**). A volcano plot was performed to identify peptides that were significantly different between the two groups (**Figure 2B**), and hierarchical clus-

Table 1. The differential peptides in the lung tissue between the HDM group and the control group

Sequence	Entry name	Start position	End position	Log FC	*P*-value
Upregulated					
ASLDKFLASVSTVLTSKYR	HBA	124	142	5.8363	0.0012
FDVSHGSAQVKGHGKKVADA	HBA	47	66	4.9625	0.0003
STSVTGSREIKSQQSEVTR	SH3L3	8	26	3.9905	0.0442
APVNVTTEVKS	EF1A1	281	291	3.3305	0.0146
TLAEKLGGSAVISLEGKPL	COF1	148	166	3.2568	0.0004
SDLHAHKLRVDPVN	HBA	85	98	3.1535	0.0107
MGQKDSYVGDEAQSKRGILT	ACTB	47	66	2.8795	0.0208
DPTSVTLKPMEIRTFLASVQWQE	MA2B1	987	1009	2.7255	0.0011
APVNVTTEVKSVE	EF1A1	281	293	2.6730	0.0005
RNDEELNKLLGRVT	H2A3	89	102	2.5934	0.0029
DSYVGDEAQSKRGILT	ACTB	51	66	2.5409	0.0490
KFDDPKFEVIDKPQS	ATP5J	94	108	2.5002	0.0069
RNDEELNKLLGKVT	H2A2A	89	102	2.4848	0.0120
NDLGEQHFKGLVLIA	ALBU	36	50	2.4092	0.0489
GRPGDRYDGMVG	HNRPK	327	338	2.2799	0.0042
PGEVMDASELEK	ZN507	859	870	2.2221	0.0387
RLLVVYPWTQRYFDSF	HBB1	31	46	2.1168	0.0077
GRLLVVYPWTQRYFDSF	HBB1	30	46	2.0929	0.0084
SVNVDYSKLKKEGPDF	NDUA4	67	82	2.0775	0.0446
SSAHFNRGPAYGLSAEV	CNN1	2	18	2.0171	0.0153
ATDELASKLSR	EFHD2	2	12	2.0032	0.0389
ASGVAVSDGVIKVFNDMKVR	COF1	2	21	2.0010	0.0421
SFPTTKTYFPH	HBA	36	46	1.9768	0.0422
VNDIFERIAGEASR	H2B1C	67	80	1.8676	0.0238
SDNQLQEGKNVI	TAGL2	163	174	1.8631	0.0416
PGVTVKDVNQQEFVRA	RS19	2	17	1.7542	0.0154
DDHDPVDKIVLQKY	ROA2	161	174	1.7297	0.0412
SLVSKGTLVQTKGTGASGSF	H13	87	106	1.6521	0.0144
PESWVPAVGLT	TSPO	2	12	1.6195	0.0320
AMVSEFLKQ	ANXA1	2	10	1.5949	0.0373
RLLLPGELAKHAVSEGTKAVTK	H2B1P	100	121	1.5213	0.0286
TEWLDGKHV	PPIA	119	127	1.5169	0.0212
ESDDSILRLAKADGIVSKNF	RS21	64	83	1.4952	0.0470
AMVSEFLKQAR	ANXA1	2	12	1.4762	0.0046
RNDEELNKLLGKVTI	H2A2A	89	103	1.4552	0.0475
ATRGTVTDFPGFDGRADAEVLR	ANXA5	2	23	1.3208	0.0145
FDITADDEPLGRVSFE	PPIA	8	23	1.3060	0.0438
SIRVTQKSYKMSTSGPRA	K2C8	2	19	1.2960	0.0305
LPETFDAREQ	CATB	80	89	1.2682	0.0273
SLGSALRPSTSRS	VIME	39	51	1.1982	0.0328
ADKPDMGEIASFDKA	TYB10	2	16	1.1841	0.0316
VEAVEQDTLQEFLKLA	SH3L3	78	93	1.1642	0.0015
SHTILLVQPTKRPEGRTY	ERH	2	19	1.1016	0.0003
AAVKTLNPKAEVARAQAA	TCPZ	2	19	1.0709	0.0322
Downregulated					
TTFKNLQTVNVDEN	RL31	112	125	-1.0154	0.0414

ATDMSQGELIHPK	HP1B3	2	14	-1.1077	0.0027
FEFADAEEDDEVKV	BORG5	396	409	-1.1170	0.0373
MDSSAVITQISKEEARGPLR	CTDS1	1	20	-1.1436	0.0148
VDSEGHLYTVP	CAV1	7	17	-1.1617	0.0339
FMDEEEEDEIRV	BORG4	338	349	-1.2078	0.0173
RTGRTGMLPANYIEFVN	LNEBL	254	270	-1.2170	0.0221
TKDDLDEEEDTHL	PODXL	491	503	-1.2238	0.0397
IVAPPGGRANITS	DPYL2	558	570	-1.2325	0.0172
GHLDDLPGALSALSDLHAH	HBA	72	90	-1.2498	0.0023
SSLLDDMTKNDPFKARVS	ZYX	153	170	-1.2803	0.0479
SYETIKEEYGVTEL	IFM2	18	31	-1.3251	0.0102
GEDAAQAEKFQHPNTDMLQ	CAVN2	2	20	-1.3471	0.0302
RAMYDYSAQDEDEVSF	LNEBL	216	231	-1.3953	0.0005
PSQMEHAMETMMLTF	S10AA	2	16	-1.4148	0.0278
MDNLSPEEVQLRAHQ	SNP23	1	15	-1.4328	0.0338
STGVPSGSSAATGSNR	VAMP3	2	17	-1.4371	0.0460
SLGSALRPSTSRSLY	VIME	39	53	-1.4392	0.0424
TEESTKENLG	TM100	2	11	-1.4765	0.0055
ADFTPAVHA	HBA	116	124	-1.5062	0.0336
SDLHAHKLRVDPVNF	HBA	85	99	-1.5388	0.0436
RSASTSGGGILVDAGYLAS	CBR2	226	244	-1.5506	0.0328
SLPVAKLPPNK	PICAL	524	534	-1.5983	0.0084
RQQLYIGSASAVAQ	SEM3E	500	513	-1.6037	0.0249
PLNTAPIQLRVREPGPPEGIQLL	RAGE	217	239	-1.6741	0.0336
GEDAAQAEKFQHPNT	CAVN2	2	16	-1.6745	0.0449
SMQPPAHLRTY	LNEBL	205	215	-1.6774	0.0283
SDAAVDTSSEITTKDLK	PTMA	2	18	-1.7189	0.0154
ASHHPADFTPAVHASLDKFLASV	HBA	111	133	-1.7693	0.0107
PGALSALSDLH	HBA	78	88	-1.7746	0.0205
GDLSSASAIMGNAKVKAHGKKVI	HBB1	47	69	-1.7792	0.0306
SIQDIENVALKSE	CALRL	444	456	-1.7818	0.0332
VDDVIKEQNRELR	CHM2B	10	22	-1.7836	0.0062
FEKTHEQLTPLVRSAGTSLVNF	APOA2	65	86	-1.8000	0.0386
GPKGVNTGAVGSYIYDKDPEGTVQP	CRIP2	184	208	-1.8159	0.0109
VLSGEDKSNIKAAWGKIGG	HBA	2	20	-1.8224	0.0190
PSQMEHAMETMMLTFHRF	S10AA	2	19	-1.8652	0.0200
SLYSSSPGGAYVTRSSAVRL	VIME	51	70	-1.9032	0.0451
FSLSGAQIDDNIPRRTTQR	DPYL2	539	557	-1.9350	0.0179
VTVTRTTITTTT	MYADM	3	14	-1.9652	0.0035
FHNPHVNPLPTGYEDE	CX6A1	96	111	-2.0137	0.0145
QEQAQEQVQPKPLES	APOA4	381	395	-2.0721	0.0372
ASHHPADFTPAVHASLDKFLAS	HBA	111	132	-2.1710	0.0446
SAEREAAEAATVAAATE	VAT1	2	18	-2.1782	0.0496
FDSTPASSTDGHSG	BORG5	140	153	-2.2264	0.0039
QIDDNIPRRTT	DPYL2	545	555	-2.2839	0.0446
AEPYDDIVGETVEKTE	MAP4	31	46	-2.3181	0.0121
SDKDPPESPVVTGVASTLK	F1142	2	20	-2.3475	0.0013
VDSEGHLYTVPIREQGNIYKPNN	CAV1	7	29	-2.4138	0.0026
GEDAAQAEKFQHPNTDM	CAVN2	2	18	-2.4174	0.0225
GTNRGASQAGMTGYGMPRQIL	TAGL2	179	199	-2.4306	0.0024

SDAAYKGVQPHVVEMDRRPGIIVA	LNEBL	154	177	-2.4320	0.0051
ERMFASFPTTKTYFPHFDVS	HBA	31	50	-2.4585	0.0051
FSLSGAQIDDNIPRRTTQ	DPYL2	539	556	-2.5835	0.0012
VREVAEEAQVAR	PRAX	195	206	-2.5919	0.0266
GPPKGPSKASSVTTF	CRIP2	105	119	-2.6767	0.0038
AGHLDDLPGALSALSDLHAH	HBA	71	90	-2.7250	0.0058
TYPGHPTSQQAGHSSPSDSAVRV	PDLI2	173	195	-2.8911	0.0137
KNPLPSKETIEQEKQAGES	TYB4	32	50	-2.8936	0.0453
ATSPQKSPLVPKSPTPKSPPS	PARVA	2	22	-2.9798	0.0154
AGLNSLEAVKRKIQALQ	TPM4	2	18	-3.2103	0.0180
SSGAHGEEGSARMWKA	CX6A1	27	42	-3.3191	0.0101
MEDVTLHIVERP	CAVN1	1	12	-3.8038	0.0013
GKIGGHGAEYGAEALERM	HBA	16	33	-3.9144	0.0131

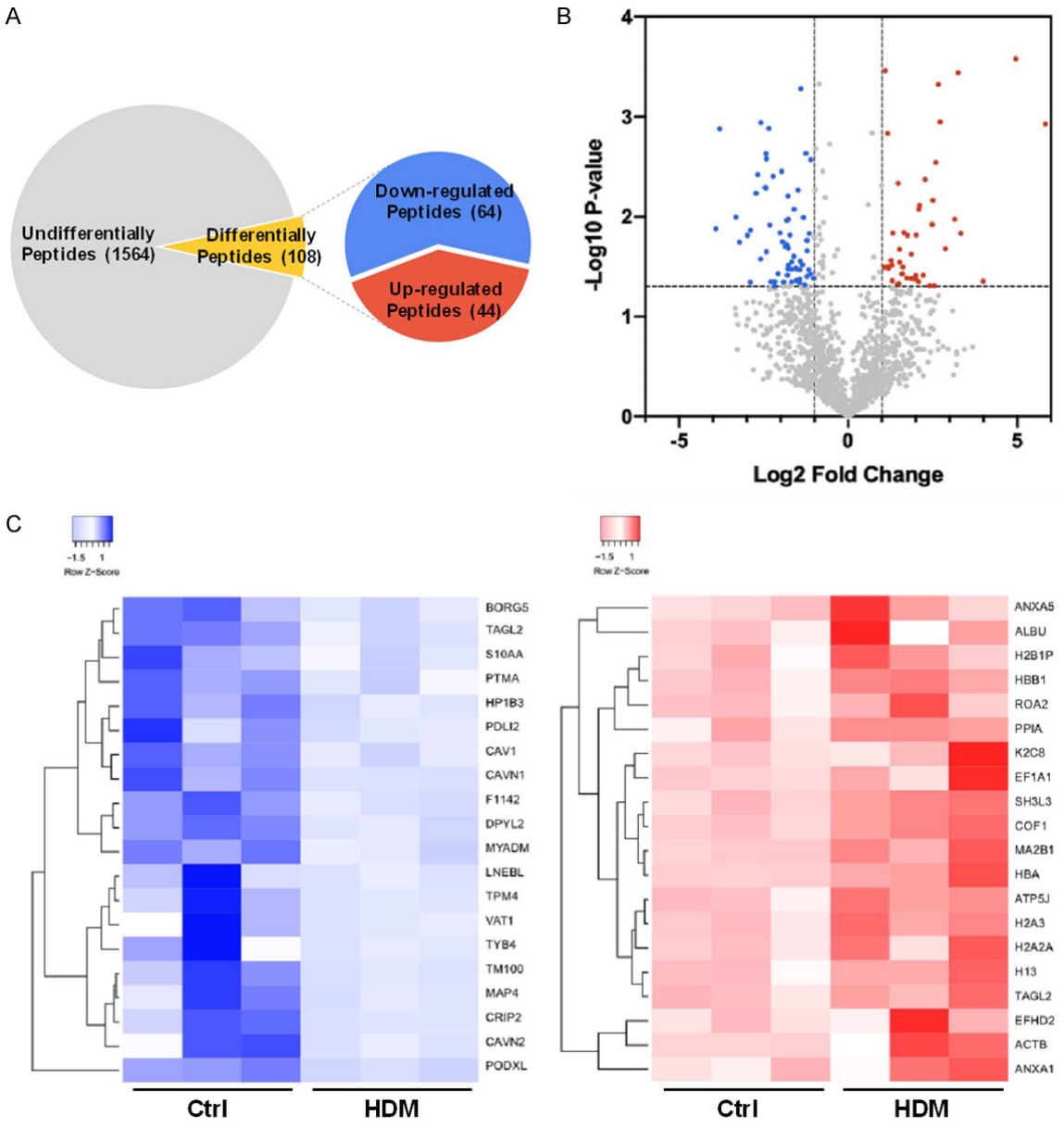

Figure 2. Differential expression of peptides between the HDM and the Control group. A. Of 1564 identified peptides, 108 peptides were significantly expressed, including 44 upregulated and 64 downregulated peptides (fold change >2 or fold change <0.5, *P*-value <0.05). B. Distribution of significantly different identified peptides visualized using volcano plot. Red dots illustrated significantly upregulated peptides in the HDM group; blue dots illustrated significantly downregulated peptides in the HDM group; grey dots illustrated the difference was not statistically significant. C. Hierarchical clustering of significantly different expression profiles between HDM group and control group. The upregulated and downregulated abundance are depicted by red and blue colors, respectively.

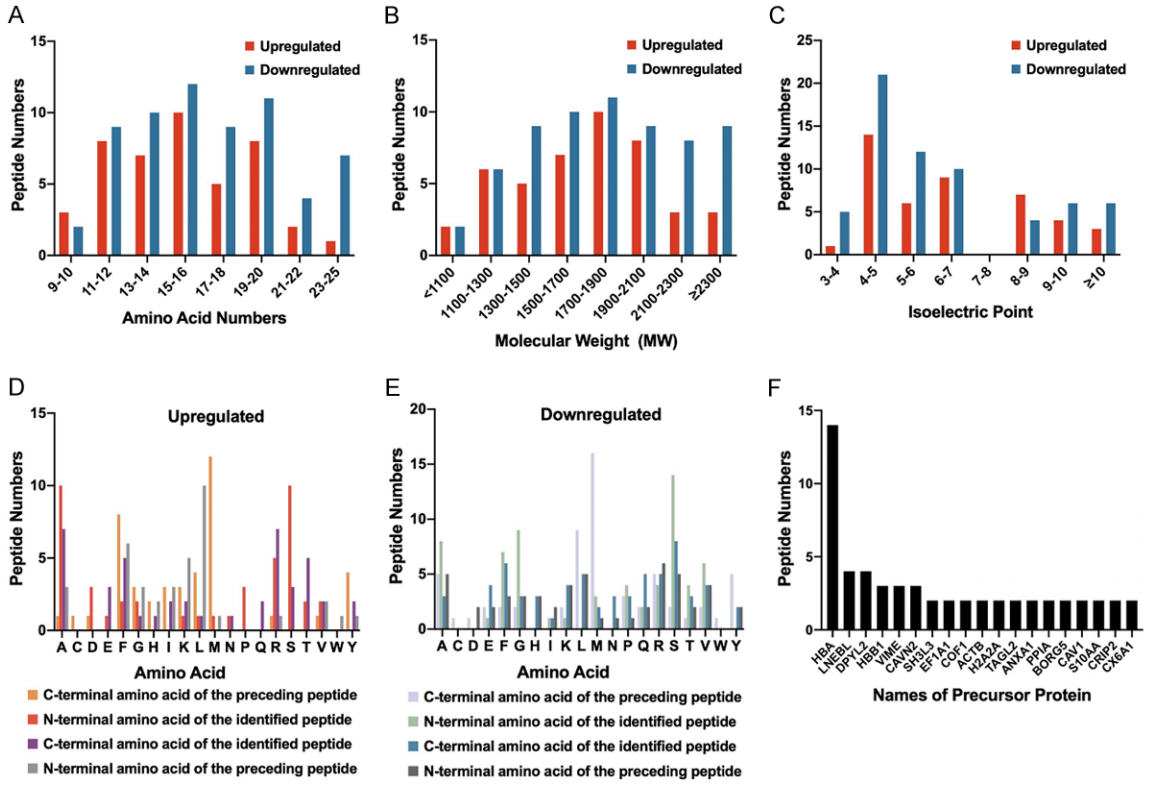

Figure 3. Features of the peptides that were significantly differentially expressed. A. Amino acids numbers of the identified peptides. B. MWs of the identified peptides. C. PI of the identified peptides. D. Cleavage sites of the N- and C-terminal in the identified peptides in the upregulated group. E. Cleavage sites of the N- and C-terminal in the identified peptides in the downregulated group. F. Peptides derived from the same precursor proteins.

tering analysis reveals the precursor protein of peptides between the two groups (**Figure 2C**).

Features of the peptides that were significantly differently expressed

The amino acid numbers ranged from 9-25 (**Figure 3A**). The MW of most identified peptides ranged from 1100-2300 Da and the PI of the peptides spread over 3.0-10.0 (**Figure 3B**, **3C**). Moreover, the peptides were determined by enzymatic cleavage to some degree, we analyzed the amino and carboxyl-terminal (N- or C-terminal) of the peptides. The cleavage sites were analyzed including the C-terminal of the preceding peptide, the N- and C-terminal of the identified peptide, and the N-terminal of the subsequent peptides (**Figure 3D**, **3E**). The common sites were alanine (A), phenylalanine (F), leucine (L), arginine (R) in the upregulated group. While in the downregulated group, the common sites were serine (S), methionine (M), alanine (A), arginine (R). Among them, hemoglobin subunit alpha (HBA) has the greatest number of related peptides (**Figure 3F**).

GO and KEGG analysis of precursors proteins

We evaluated the GO biological and KEGG pathway analysis to predict the underlying functions of the precursor proteins. Biological progress, cellular component, and molecular function

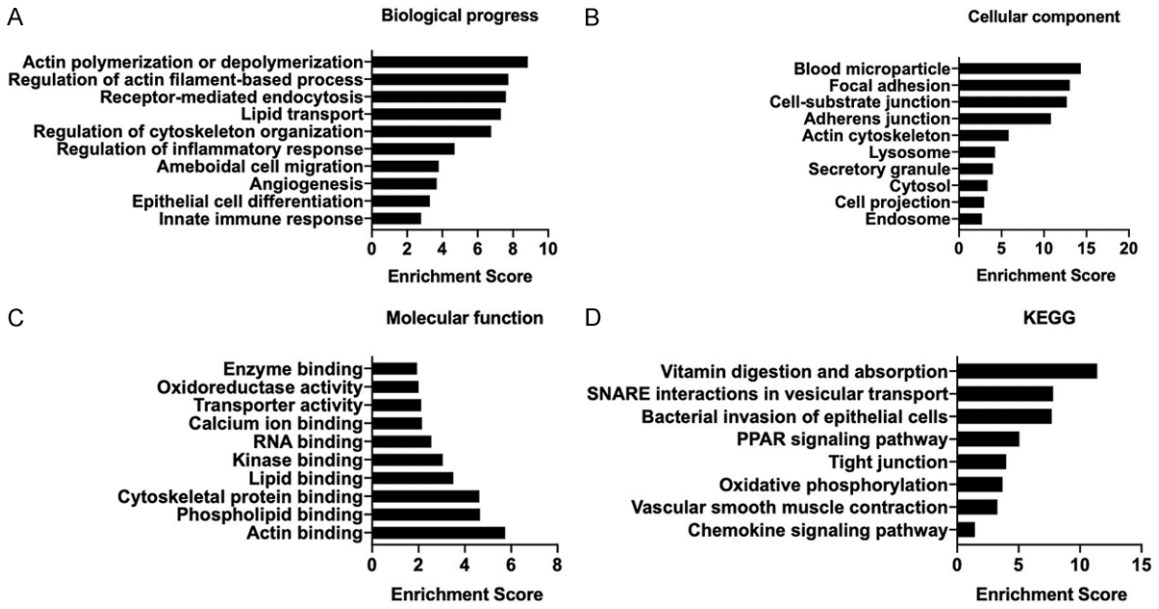

Figure 4. GO and KEGG pathway analysis of the precursor proteins. A. Biological process. B. Cellular component. C. Molecular function. D. KEGG signaling pathways.

were evaluated by enrichment analysis. For biological progress, the most highly enriched categories were actin polymerization or depolymerization, regulation of actin filament-based process, receptor-mediated endocytosis (RME), and lipid transport (**Figure 4A**). As for cellular components, blood microparticle, focal adhesion, cell-substrate junction, adherens junction, and actin cytoskeleton were most populated (**Figure 4B**). For molecular functions, binding of actin, phospholipid, and cytoskeletal protein were the highly enriched subcategories (**Figure 4C**). The precursors proteins of identified peptides were involved in vitamin digestion and absorption, soluble N-ethylmaleimide-sensitive factor attachment protein receptor (SNARE) interactions in vesicular transport, bacterial invasion of epithelial cells, PPAR signaling pathway, tight junction, oxidative phosphorylation, vascular smooth muscle contraction, and chemokine signaling pathways by KEGG pathway analysis (**Figure 4D**).

Association networks analysis of functional proteins

We use the STRING database to analyze protein-protein interactions of the corresponding precursor proteins (**Figure 5**). We performed a western blot analysis of E-cadherin as an EMT marker (**Figure 6**). The expression of E-cadherin is downregulated in the HDM group. Then we use the UniProt database to analyze the functional domains (**Table 2**). We found that the upregulated peptides "STSVTGSREIKSQQSEVTR" and "VEAVEQDTLQEFLKLA" developed from the functional domain of glutaredoxin might be related to the pathophysiological process of asthma. Peptide "STSVTGSREIKSQQSEVTR" shared 100% identity of the amino acid sequence with humans and peptide "VEAVEQDTLQEFLKLA" shared 93.8% identity of the amino acid sequence with humans (**Figure 7A**, **7C**).

Discussion

Asthma is a major global health concern. In the year of 2015, there were four hundred thousands of people who died from asthma [15]. Allergic asthma is the most frequent phenotype of asthma, which is characterized by sensitization to an allergen and Th2-mediated immune response [16]. The main feature of allergic asthma contains chronic eosinophilic inflammation and remodeling of the airway, leading to hyperplasia of smooth muscle mass, subepithelial fibrosis, and goblet cell hyperplasia [17]. In our study, we used the solution of HDM to construct the asthmatic mouse model. Histological analysis of lung sections showed increased eosinophils infiltration in the lamina propria, basal layer and submucosa, and thickening of the bronchial wall, swelling and hyper-

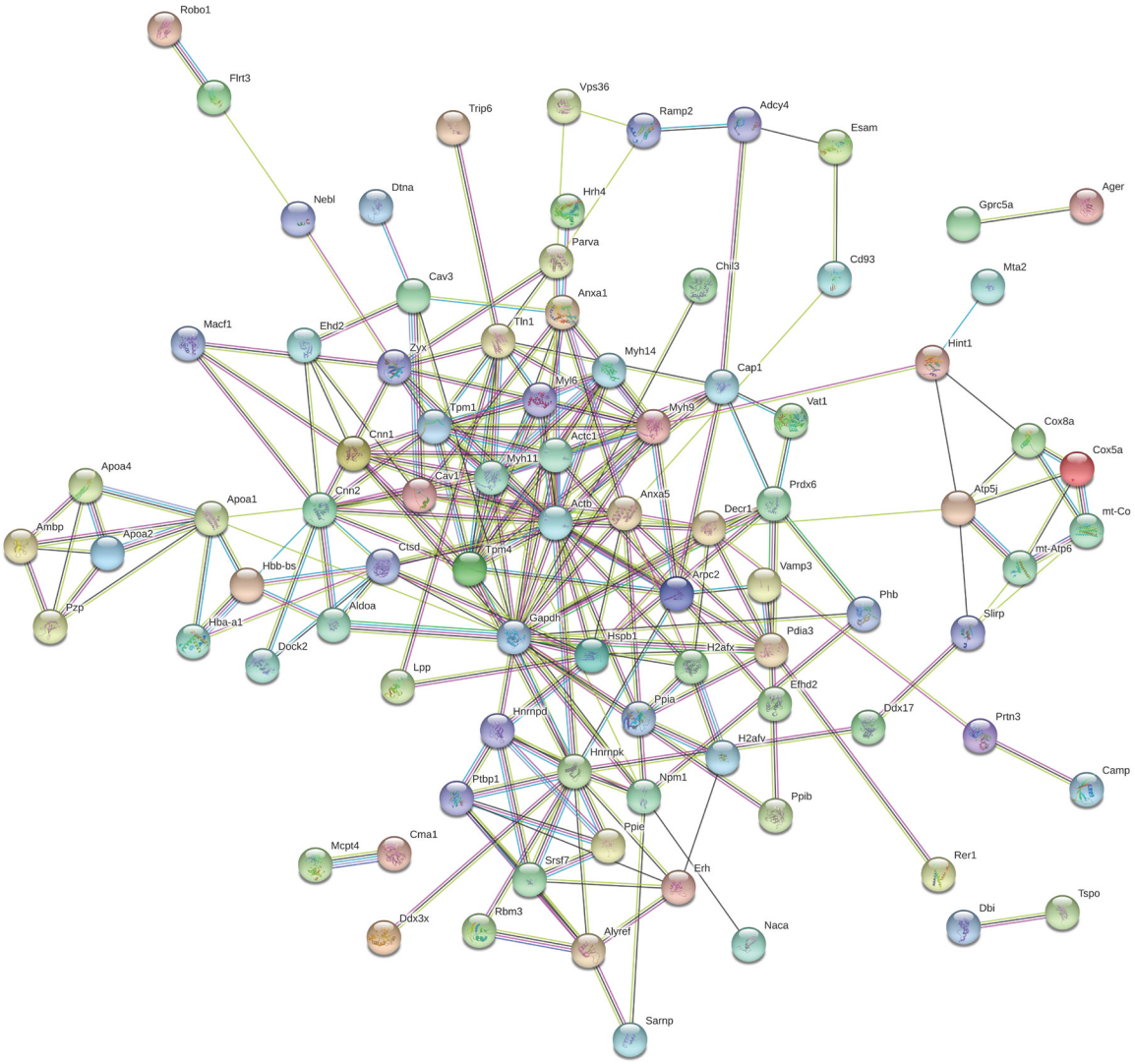

Figure 5. Association networks analysis of functional proteins. The STRING database was used to predict the protein-protein interaction associated with differential expression peptides. Network nodes mean proteins, and the edge represents the predicted functional associations.

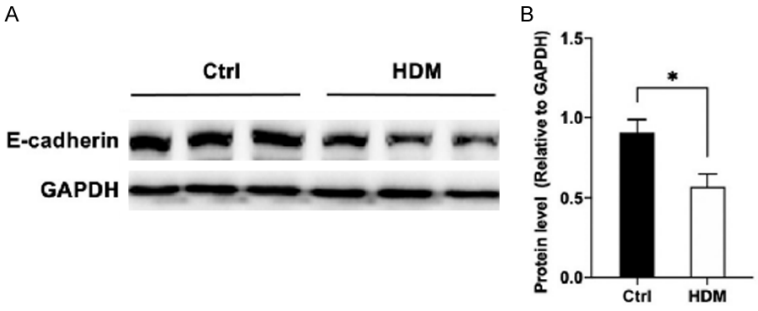

Figure 6. The involvement of epithelial-mesenchymal transition (EMT) in lung tissues of asthmatic mice and controls. A. Western blot analysis of E-cadherin as an EMT marker. B. Protein levels of E-cadherin relative to GAPDH. **P*-value <0.05.

emia of the mucosa. Previous studies reported that peptides can play a therapeutic role in asthma through modulating the immune response [8]. But the underlying molecular mechanisms by which peptides contribute to the pathogenesis of asthma have not been elucidated.

We attempted to identify novel peptides in asthma pathogenesis by comparing the peptid-

Table 2. Peptides from functional domains

Peptide sequence	Protein IDs	Position	Domain	Description	Cellular location
Upregulated					
STSVTGSREIKSQQSEVTR	Q91VW3	8-26	2-93	Glutaredoxin	Nucleus, Cytoplasm
NDLGEQHFKGLVLIA	P07724	36-50	19-211	Albumin 1	Extracellular region or secreted
DDHDPVDKIVLQKY	O88569	161-174	112-191	RRM2	Extracellular region or secreted
SLVSKGTLVQTKGTGASGSF	P43277	87-106	37-110	H15	Nucleus, Chromosome
TEWLDGKHV	P17742	119-127	7-163	PPIase cyclophilin-type	Extracellular region or secreted
FDITADDEPLGRVSFE	P17742	8-23	7-163	PPIase cyclophilin-type	Extracellular region or secreted
VEAVEQDTLQEFLKLA	Q91VW3	78-93	2-93	Glutaredoxin	Nucleus, Cytoplasm
Downregulated					
VDSEGHLYTVP	P49817	7-17	2-94	Required for homooligomerization	Cell membrane, Golgi apparatus membrane
RTGRTGMLPANYIEFVN	Q9DC07	254-270	210-270	SH3	Cytoplasm
RAMYDYSAQDEDEVSF	Q9DC07	216-231	210-270	SH3	Cytoplasm
RQQLYIGSASAVAQ	P70275	500-513	32-516	Sema	Extracellular region or secreted
VDSEGHLYTVPIREQGNIYKPNN	P49817	7-29	2-94	Required for homooligomerization	Cell membrane, Golgi apparatus membrane

omic profiles of lung tissues from the HDM-induced mouse model and the controls. We identified 108 differentially expressed peptides that were originated from 70 proteins. The MW is less than 3000 Dalton in all the identified peptides and most of the PI were distributed from 4.0 to 7.0. The PI near the middle position is a blank area. It is well known that bioactive peptides are mainly derived from the cleavage of proteins [18]. The ubiquitin-proteasome system worked for most of the cytoplasmic proteins. Proteasome destruct proteins after tagged by enzyme-mediated poly-ubiquitination, and the different substrate cleavage site may cause altered peptide products [19]. The peptides developed from corresponding protein domains can exhibit biological activities [18], and partly retains the original functions of their precursor proteins. Thus, we could predict the potential functions of peptides through functional analysis of precursor proteins. The GO analysis demonstrated that the function of precursor proteins was mainly enriched in actin polymerization or depolymerization (CFL1, SH3BGRL3, CDC42EP1, CDC42EP4, and MYADM), regulation of actin filament-based process (SEMA3E, S100A10, CFL1, SH3BGRL3, CDC42EP1, CAV1, CDC42EP4, and MYADM), RME (CAV1, CALCRL, HNRNPK, and PICALM) and regulation of inflammatory response (RPS19, CALCRL, AGER, and ANXA1). Molecular function focused on actin binding (TMSB10, CFL1, CNN1, PARVA, TPM4, TMSB4X, and NEBL). KEGG analysis showed that the precursor proteins focus on SNARE interactions in vesicular transport (VAMP3 and CAMP) and tight junction (ACTB, MYH9, MYH11, and MYH14) signaling pathways.

GO and KEGG analysis demonstrated that the functions focused on the regulation of actin, which takes part in the migration of eosinophils into tissues [20] and airway remodeling. The changes like epithelial-mesenchymal transition (EMT) in the bronchial epithelial cells, smooth muscle hyperplasia, and enhanced vascularity led to airway remodeling in asthma [21]. It was reported that α-smooth muscle actin increased under the process of EMT in BEAS-2B cells, and actin-associated proteins participate in airway remodeling by regulating actin cytoskeleton in airway smooth muscle in asthma [22]. Actin-associated proteins were reported to participate in airway remodeling by regulating actin cytoskeleton in airway smooth muscle [23]. Studies found that replenishment of semaphorin 3E (Sema3E) could reduce eosinophilic inflammation and the expression of angiogenesis markers in the asthmatic mouse model [24, 25], inhibit proliferation, and migration of human airway smooth muscle cells by F-actin depolymerization [26]. Immune response activation is also the main characteristic of asthma pathology. Cells could absorb macromolecules such as peptides, cytokines, bacteria, and viruses by budding inwards through the plasma membrane by RME [27]. The internalization of RME initiates the processing of antigens, then recognized by the cells of the adaptive immune system. As a barrier against invading patho-

A

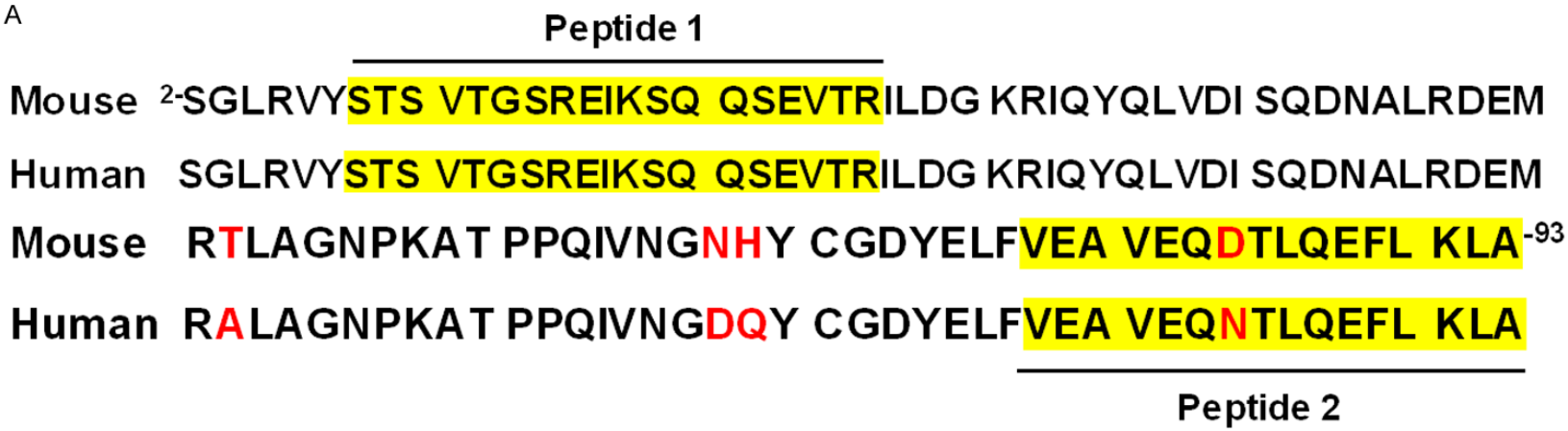

B

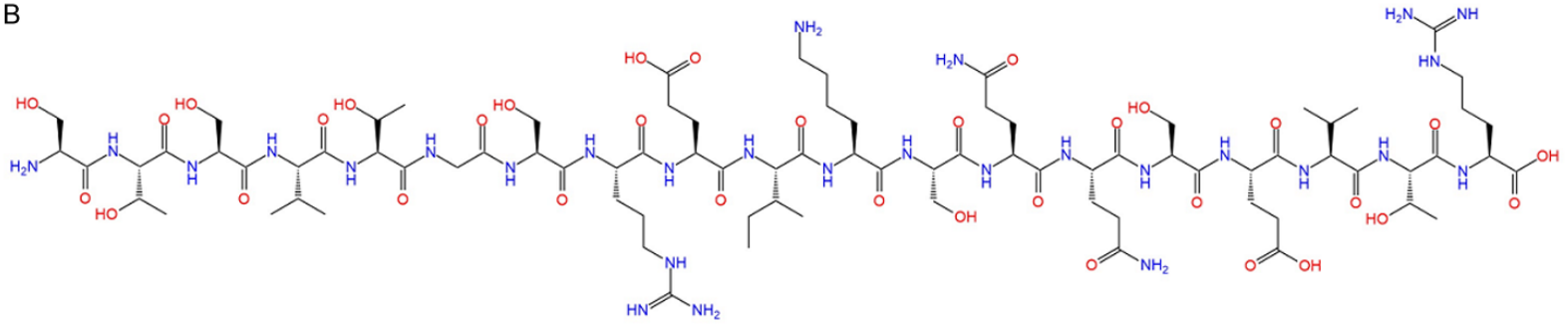

C

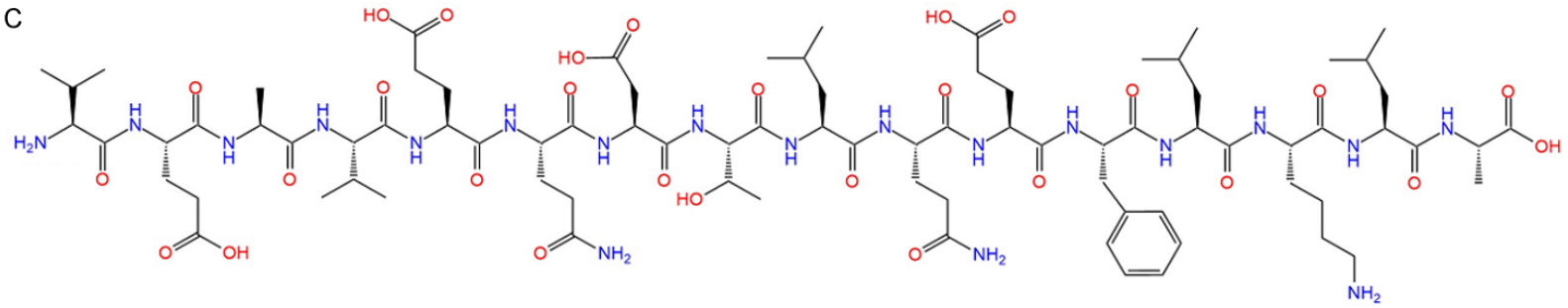

Figure 7. The functional domain and molecular formula of peptides. A. Peptides derived from the functional domain in mice and humans. B. Molecular formula of STSVTGSREIKSQQSEVTR. C. Molecular formula of VEAVEQDTLQEFLKLA.

gens, the airway epithelium could activate downstream signaling by recognizing inhaled microbes and allergens, then activate the immune system by promoting the release of inflammatory cytokines or chemokines [17]. It has been known that peptides could treat asthma by regulating the immune response. For example, a peptide that targets the phosphorylation site of myristoylated alanine-rich C kinase substrate was proved to be efficacious against steroid-resistant asthma through inhibiting neutrophilic inflammation [28]. Peptide SJMHE1 treatment suppressed airway inflammation in ovalbumin-sensitized mice through downregulating Th2 immune responses and upregulating Th1 and Tregs immune responses [29]. A hybrid peptide which is composed of neurotensin and endomorphin-2 pharmacophores could inhibit 2, 4-dinitrofluorobenzene induced inflammatory cells infiltration and NF-κB signal pathway in mice model to regulate inflammation in asthma [30].

Precursor proteins analysis revealed that peptides derived from these certain proteins, including heterogeneous ribonucleoprotein K (HNRNPK) [31], myosin light chain 6 (Myl6) [32], and Annexin A1 (ANXA1) [33] may be related to the incidence of asthma. Then we use the UniProt database to analyze the peptides originated from functional domains of their precursor proteins. As a member of the thioredoxin-like protein superfamily, SH3 domain binding glutamic acid-rich protein-like 3 (SH3BGRL3) is conformed to chromosome 1p34.3-3512095696 with the structure of 1.6 angstrom resolution crystal [34]. Peptides "STSVTGSREIKSQQSEVTR" and "VEAVEQDTLQEFLKLA" from the functional domain of SH3BGRL3 share homology between the human and mouse. In urothelial carcinoma, SH3BGRL3 stable cancer cells show the loss of cohesiveness by upregulating EMT markers in vitro [35]. Our data suggested that these two peptides may be involved in asthma pathology, implying the potential function of impacting EMT progress.

Our studies still had some shortcomings. We only focused on animal models, so the conclusions couldn't be completely generalizable to humans directly. There are still some non-allergic types of asthma, for those patients, the pathogenesis is different from allergic asthma. Further validation of the two peptides of SH3BGRL3 is also required.

Conclusions

Our study focused on differentially expressed peptides preliminarily with LC-MS/MS using lung tissues from HDM-induced mice model and controls. Through the analysis of peptides and their precursor proteins, we found some peptides that were associated with the pathogenesis of asthma. This study will be useful for applications of peptides and find out new therapeutic targets in asthma.

Acknowledgements

Our study was supported by International Science and Technology Cooperation Project of Shanghai Science and Technology Commission (18410721300) and the National Natural Science Foundation of China (81901512, 81774365).

Disclosure of conflict of interest

None.

Address correspondence to: Xiaoyan Dong, Department of Respiratory, Shanghai Children's Hospital, Shanghai Jiao Tong University, No. 355, Luding Road, Shanghai 200062, China. Tel: +86-18930734642; E-mail: dongxy@shchildren.com.cn; Xingyun Wang, Hongqiao International Institute of Medicine, Tongren Hospital, Shanghai Jiao Tong University School of Medicine, No. 720, Xianxia Road, Shanghai 200336, China. Tel: +86-182626-36297; E-mail: xyw@njmu.edu.cn

References

[1] GBD Chronic Respiratory Disease Collaborators. Prevalence and attributable health burden of chronic respiratory diseases, 1990-2017: a systematic analysis for the global burden of disease study 2017. Lancet Respir Med 2020; 8: 585-596.

[2] Holgate ST. Pathogenesis of asthma. Clin Exp Allergy 2008; 38: 872-897.

[3] Elieh Ali Komi D and Bjermer L. Mast cell-mediated orchestration of the immune responses in human allergic asthma: current insights. Clin Rev Allergy Immunol 2019; 56: 234-247.

[4] Holgate ST, Wenzel S, Postma DS, Weiss ST, Renz H and Sly PD. Asthma. Nat Rev Dis Primers 2015; 1: 15025.

[5] Peters MC and Wenzel SE. Intersection of biology and therapeutics: type 2 targeted therapeutics for adult asthma. Lancet 2020; 395: 371-383.

[6] DiMango E, Serebrisky D, Narula S, Shim C, Keating C, Sheares B, Perzanowski M, Miller R, DiMango A, Andrews H, Merle D, Liu X, Calatroni A and Kattan M. Individualized household allergen intervention lowers allergen level but not asthma medication use: a randomized controlled trial. J Allergy Clin Immunol Pract 2016; 4: 671-679 e674.
[7] Han J, Nguyen J, Kim Y, Geng B, Romanowski G, Alejandro L, Proudfoot J, Xu R and Leibel S. Effect of inhaled corticosteroid use on weight (BMI) in pediatric patients with moderate-severe asthma. J Asthma 2019; 56: 263-269.
[8] Tian L, Li W, Wang J, Zhang Y, Zheng Y, Qi H, Guo X, Zhang Y, Ma D, Shen H and Wang Y. The CKLF1-C19 peptide attenuates allergic lung inflammation by inhibiting CCR3- and CCR4-mediated chemotaxis in a mouse model of asthma. Allergy 2011; 66: 287-297.
[9] Viby NE, Pedersen L, Lund TK, Kissow H, Backer V, Nexo E, Thim L and Poulsen SS. Trefoil factor peptides in serum and sputum from subjects with asthma and COPD. Clin Respir J 2015; 9: 322-329.
[10] Lange-Consiglio A, Stucchi L, Zucca E, Lavoie JP, Cremonesi F and Ferrucci F. Insights into animal models for cell-based therapies in translational studies of lung diseases: is the horse with naturally occurring asthma the right choice? Cytotherapy 2019; 21: 525-534.
[11] Kianmeher M, Ghorani V and Boskabady MH. Animal model of asthma, various methods and measured parameters: a methodological review. Iran J Allergy Asthma Immunol 2016; 15: 445-465.
[12] Aun MV, Bonamichi-Santos R, Arantes-Costa FM, Kalil J and Giavina-Bianchi P. Animal models of asthma: utility and limitations. J Asthma Allergy 2017; 10: 293-301.
[13] Jia Z, Bao K, Wei P, Yu X, Zhang Y, Wang X, Wang X, Yao L, Li L, Wu P, Yuan W, Wang S, Zheng J, Hua Y and Hong M. EGFR activation-induced decreases in claudin1 promote MUC5AC expression and exacerbate asthma in mice. Mucosal Immunol 2021; 14: 125-134.
[14] Debeuf N, Haspeslagh E, van Helden M, Hammad H and Lambrecht BN. Mouse models of asthma. Curr Protoc Mouse Biol 2016; 6: 169-184.
[15] GBD Chronic Respiratory Disease Collaborators. Global, regional, and national deaths, prevalence, disability-adjusted life years, and years lived with disability for chronic obstructive pulmonary disease and asthma, 1990-2015: a systematic analysis for the Global Burden of Disease Study 2015. Lancet Respir Med 2017; 5: 691-706.
[16] Boonpiyathad T, Sozener ZC, Satitsuksanoa P and Akdis CA. Immunologic mechanisms in asthma. Semin Immunol 2019; 46: 101333.
[17] Heijink IH, Kuchibhotla VNS, Roffel MP, Maes T, Knight DA, Sayers I and Nawijn MC. Epithelial cell dysfunction, a major driver of asthma development. Allergy 2020; 75: 1902-1917.
[18] Polonelli L, Ciociola T, Sperinde M, Giovati L, D'Adda T, Galati S, Travassos LR, Magliani W and Conti S. Fungicidal activity of peptides encoded by immunoglobulin genes. Sci Rep 2017; 7: 10896.
[19] Liepe J, Holzhutter HG, Bellavista E, Kloetzel PM, Stumpf MP and Mishto M. Quantitative time-resolved analysis reveals intricate, differential regulation of standard- and immunoproteasomes. Elife 2015; 4: e07545.
[20] Barnard R, Barnard A, Salmon G, Liu W and Sreckovic S. Histamine-induced actin polymerization in human eosinophils: an imaging approach for histamine H4 receptor. Cytometry A 2008; 73: 299-304.
[21] Banno A, Reddy AT, Lakshmi SP and Reddy RC. Bidirectional interaction of airway epithelial remodeling and inflammation in asthma. Clin Sci (Lond) 2020; 134: 1063-1079.
[22] Thevenot PT, Saravia J, Jin N, Giaimo JD, Chustz RE, Mahne S, Kelley MA, Hebert VY, Dellinger B, Dugas TR, Demayo FJ and Cormier SA. Radical-containing ultrafine particulate matter initiates epithelial-to-mesenchymal transitions in airway epithelial cells. Am J Respir Cell Mol Biol 2013; 48: 188-197.
[23] Tang DD. Critical role of actin-associated proteins in smooth muscle contraction, cell proliferation, airway hyperresponsiveness and airway remodeling. Respir Res 2015; 16: 134.
[24] Movassagh H, Shan L, Duke-Cohan JS, Halayko AJ, Uzonna JE and Gounni AS. Semaphorin 3E alleviates hallmarks of house dust mite-induced allergic airway disease. Am J Pathol 2017; 187: 1566-1576.
[25] Tatari N, Movassagh H, Shan L, Koussih L and Gounni AS. Semaphorin 3E inhibits house dust mite-induced angiogenesis in a mouse model of allergic asthma. Am J Pathol 2019; 189: 762-772.
[26] Movassagh H, Shan L, Halayko AJ, Roth M, Tamm M, Chakir J and Gounni AS. Neuronal chemorepellent semaphorin 3E inhibits human airway smooth muscle cell proliferation and migration. J Allergy Clin Immunol 2014; 133: 560-567.
[27] Kornilova ES. Receptor-mediated endocytosis and cytoskeleton. Biochemistry (Mosc) 2014; 79: 865-878.
[28] Wang CN, Lin YC, Chang BC, Chen CH, Wu R and Lee CC. Targeting the phosphorylation site of myristoylated alanine-rich C kinase substrate alleviates symptoms in a murine model of steroid-resistant asthma. Br J Pharmacol 2019; 176: 1122-1134.

[29] Zhang W, Li L, Zheng Y, Xue F, Yu M, Ma Y, Dong L, Shan Z, Feng D, Wang T and Wang X. Schistosoma japonicum peptide SJMHE1 suppresses airway inflammation of allergic asthma in mice. J Cell Mol Med 2019; 23: 7819-7829.

[30] Russjan E, Andrzejewski K, Sulejczak D, Kleczkowska P and Kaczynska K. Endomorphin-2- and neurotensin-based chimeric peptide attenuates airway inflammation in mouse model of nonallergic asthma. Int J Mol Sci 2019; 20: 5935.

[31] Wong SL, To J, Santos J, Allam V, Dalton JP, Djordjevic SP, Donnelly S, Padula MP and Sukkar MB. Proteomic analysis of extracellular HMGB1 identifies binding partners and exposes its potential role in airway epithelial cell homeostasis. J Proteome Res 2018; 17: 33-45.

[32] Zhu Z, Guo Y, Shi H, Liu CL, Panganiban RA, Chung W, O'Connor LJ, Himes BE, Gazal S, Hasegawa K, Camargo CA Jr, Qi L, Moffatt MF, Hu FB, Lu Q, Cookson WOC and Liang L. Shared genetic and experimental links between obesity-related traits and asthma subtypes in UK Biobank. J Allergy Clin Immunol 2020; 145: 537-549.

[33] Ng FS, Wong KY, Guan SP, Mustafa FB, Kajiji TS, Bist P, Biswas SK, Wong WS and Lim LH. Annexin-1-deficient mice exhibit spontaneous airway hyperresponsiveness and exacerbated allergen-specific antibody responses in a mouse model of asthma. Clin Exp Allergy 2011; 41: 1793-1803.

[34] Nardini M, Mazzocco M, Massaro A, Maffei M, Vergano A, Donadini A, Scartezzini P and Bolognesi M. Crystal structure of the glutaredoxin-like protein SH3BGRL3 at 1.6 angstrom resolution. Biochem Biophys Res Commun 2004; 318: 470-476.

[35] Chiang CY, Pan CC, Chang HY, Lai MD, Tzai TS, Tsai YS, Ling P, Liu HS, Lee BF, Cheng HL, Ho CL, Chen SH and Chow NH. SH3BGRL3 protein as a potential prognostic biomarker for urothelial carcinoma: a novel binding partner of epidermal growth factor receptor. Clin Cancer Res 2015; 21: 5601-5611.